EFFECTS OF BENDING ON THE OPTOELECTRONIC PROPERTIES AND FAILURE MECHANISM IN ORGANIC PHOTOVOLTAICS

A

THESIS

Presented to the Department of Theoretical Physics

The African University of Science and Technology (AUST)

In Partial Fulfilment of the Requirement for the Degree of

MASTER OF SCIENCE

By

ASARE JOSEPH

Abuja, Nigeria

DECEMBER, 2011

ABSTRACT

This research investigates the effects of bending on the electrical, optical, structural and mechanical properties of flexible organic photovoltaic (OPV) cells. Bulk heterojunction organic solar cells were fabricated on Polyethylene terephthalate (PET) substrates using Poly-3-hexylthiophene: [6, 6]-phenyl-C61-butyric acid methyl ester (P3HT: PCBM) as the active layer and Poly (3, 4-ethylenedioxythiophene) Polystyrenesulfonate (PEDOT: PSS) as the hole injection layer. All the organic layers were deposited by spin coating while the Al cathode was vacuum thermally evaporated. The Indium Tin Oxide (ITO) anode has an average optical transmittance of 85% in the visible spectrum, a sheet resistivity of 60 ohms per square and an average surface roughness of 3nm. The relationship between the optoelectronic performance of the various device layers and the applied mechanical strains has been analyzed. The effects of stress and strain on the current-voltage characteristics of the device and its failure were modeled using the Abaqus software.

DEDICATION

I dedicate this work to my Father Jehovah Elohim and my best friend the Holy Spirit.

ACKNOWLEDGEMENT

I would like to show my first and deepest appreciation to the Almighty God for making this thesis a success. Secondly, to Prof Wole Soboyejo and Dr. Zebese Kana, I would like to show my sincere and heartfelt gratitude to them for their supervision over this thesis work. I acknowledge Dr Shola Odusanya, Dr Joseph Berry, Dr Tudor Popov, Prof Jean Chabi O., Dr Nimah Rabah, Jing Du and all my lecturers for their help, support and influence during my stay in both SHESTCO (Sheda Science and Technology Complex) and AUST (African University of Science and Technology).

I appreciate the World Bank Step-B SHESTCO AUST programme for releasing the needed funds to facilitate the progress of this research. Moreover, I acknowledge the Physics Advance Laboratory staff for their immerse support in this thesis work especially Joseph Ogbonnaya Uduma, Oladipupo Olayinka Samuel, Onugukeyna Oluchukwu, K. K. Adama, Blessing Omaji, Olalekan Deborah, and Mrs Umwana Iwok. The next acknowledgement goes to Eng. Matthew, Eng. Atandah, Ezekiel (IT) and Nelson (IT) from the Mechanical section of SHESTCO. I salute Eng. Gadu Adamah (GIF) for his assistance during my work at GIF; I am extremely indebted to him. My heartfelt thanks again go to my family back home for their support throughout my Masters programme.

Finally, I would like to acknowledge Eric Mensah Amarfio, Adebayo Fashina, Isaiah Moses, Ivy Asuo, Kofi Ampaw E., Johnson, Kehinde O., Mr Biodum, Titus N., Azeb D., Selasie Enty G., Alice O., Nsima J., Tracey O., Nutifafa E. Y., Kakra O. D., Juliet Sackey, Jonas Bugase, Yiporo, Damilola Y., Vitalis C., Olem M. N. and all my colleagues for their unfailing kindness, love, help and care whiles on campus.

TABLE OF CONTENT

LIST OF FIGURES

LIST OF TABLES

CHAPTER ONE

INTRODUCTION

1.1 Introduction

The Global consumption of energy on the earth surface is estimated to be 15TW. 32TW is the total geothermal energy available, 870TW is that of wind and direct solar offers up to 86,000TW [1]. With these statistics, solar energy would be the ultimate source of fuel due to its abundance in availability. Ultimately, solar energy would replace the dwindling fossil fuels' reserves in this new era of cleaner and more efficient energy as the world surges on to new technologies and horizons.

1.2 The Solar Cell

A solar cell is a semiconductor PN junction diode, normally without an external bias, that provides electrical power to a load when illuminated as shown in figure below. Solar cells or photovoltaic devices are devices that can convert efficiently the energy in sunlight into usable electrical energy.

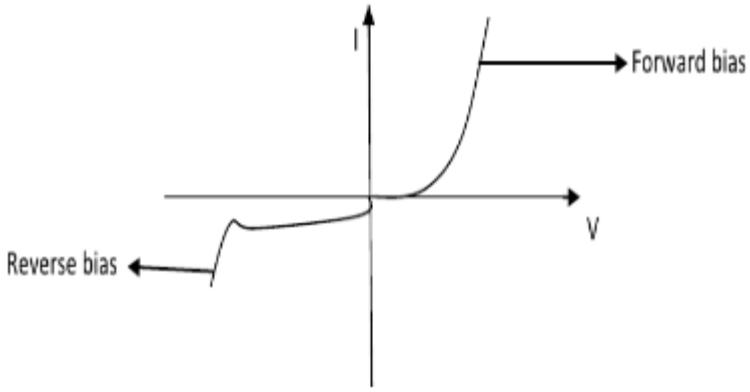

Figure 1.1: Current Voltage (IV) characteristics of a PN junction diode

A solar cell under illumination would exhibit the IV characteristics of a forward bias PN junction diode as indicated in the Figure 1.2:

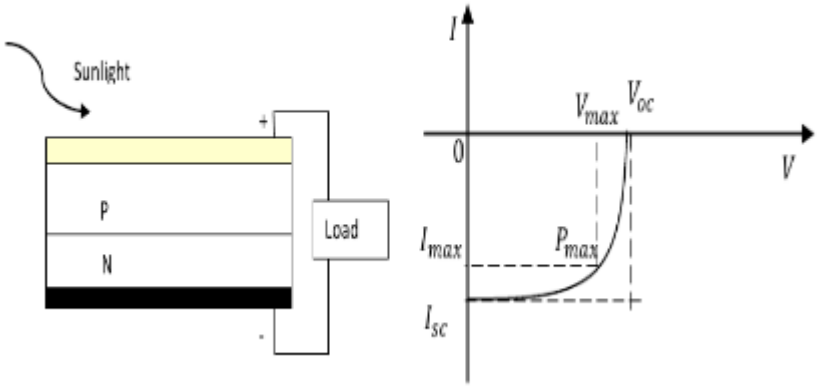

Figure 1.2: Characteristics of a solar cell under light

In the dark, a solar cell would exhibit the Ohmic characteristics curve of a conventional resistor. The efficiency of a solar cell is the ratio of the electrical power it delivers to the

load, to the optical power incident on the cell. Maximum efficiency is when power delivered to the load is P_{max} [2].

A solar cell could be either organically or inorganically manufactured. A solar cell made by depositing one or more layers (thin films) of photovoltaic materials on a substrate is called a thin- film photovoltaic cell (TFPV) or thin- film solar cell (TFSC). These have thickness ranges varying from a few nanometers to tens of micrometers. Various deposition methods on a variety of substrates are used to deposit many different many different photovoltaic materials. Therefore the photovoltaic material used categorizes the thin- film solar cell into inorganic and organic forms given as:

1. Amorphous Silicon and other thin- film Silicon
2. Cadmium Telluride } Inorganic
3. Copper Indium Gallium Selenide
4. Dye synthesized solar cell and other organic sollar cells [3]

1.2.1 Inorganic Solar Cell Limitations

There has been increasing interest in the development of low cost organic electronic devices stimulated by the potential for significant processing cost reductions compared to the cost of their amorphous or crystalline silicon counterparts in solar cell and light- emitting devices [4]. Organic electronics has become a vastly developed field in the past two decades due to their promise of low cost, lightweight, versatility of chemical design and synthesis, ease of processing, and mechanical flexibility as compared to inorganic solar cells [5]. The main advantages of the organic semiconductors over inorganic semiconductors in the electronic industry are: easier deposition of thin films, higher degree of sensi-

tivity to external agents, a potential lower- cost on large scale production, higher absorption coefficient and greater flexibility [6]. However, the major merit is that very simple and low cost deposition techniques such as; vacuum evaporation, spin coating and the like are used to deposit these organic thin films on some suitable substrates be it glassy or flexible.

1.3 Organic Electronics

The make-up of an electronic device could also be either inorganic or organic. Examples of organic electronics are light-emitting diodes (OLEDs), field- effect transistors (OFETs), solar cells and photo-detectors (Organic Photovoltaics- OPVs). Organic electronics are now applicable to PV technology to solve the growing energy challenges that will take an integral part in future energy production. However, organic electronic devices' performance and lifetime such as that of OPV depend critically on the properties of the active materials used and their interfaces. An example is how surface energy and work-function greatly affect the charge injection or extraction and transport in organic semiconductors which has been explained further in chapter 2 [5]. Recent improvements in efficiency from ~1% to 8.3%[7] has strengthened the case for organic photovoltaic (OPV) cells thus bringing them closer to commercialization and suggesting that organic electronic devices may evolve to be widely used in both rural and urban applications. Figure 1.3 below shows the schematics of an organic solar cell manufactured in the electronic industries.

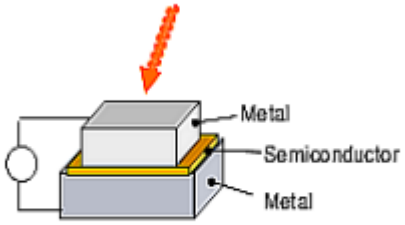

Figure 1.3: The Schematics of an organic photovoltaic cell [Adapted from Korhan Demirkan]

1.4 Photovoltaic Energy Conversion

The ability to do the work of forcing electrons to move especially from the valence band to the conduction band is what is termed as the potential difference or Voltage. The potential difference across a conductor such as copper, silver and gold (they have one valence electron- good conductors) causes current to flow thereby providing electricity (see Figure 1.4)[8]. The conversion of electromagnetic energy such as light (which includes infra-red, visible and ultraviolet) to electric energy in the form of current or voltage is termed photovoltaic energy conversion [9].

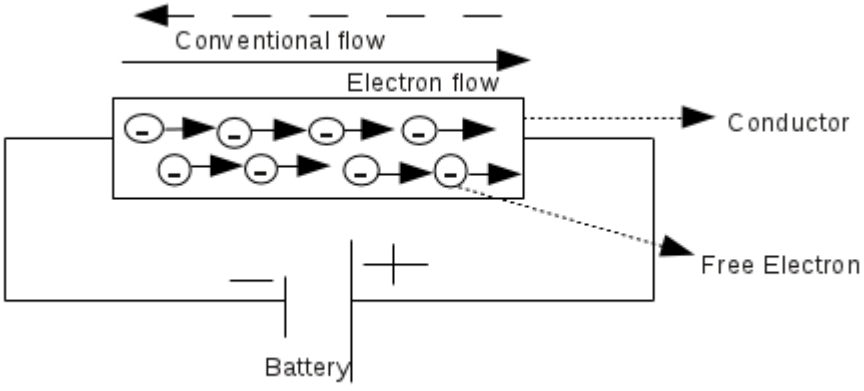

Figure 1.4: Electricity generation [8]

1.4 The Make Up of a Photovoltaic Cell

When the light is incident on the absorber/ material, it experiences a transition from a ground state to an excited state after which this excited state is converted to free negative and positive charge carrier pairs. The free negative charge carrier moves to the cathode whiles the free positive charge carrier move to the anode. During this discriminating transport mechanism, the energetic photo-generated negative charge carriers arriving at the cathode result in electrons which move through an electric circuit losing their energy to electrical loads as they make their way back to the anode to recombine with the arriving positive charge carriers. This recombination process eventually returns the absorber back to its ground state [9].

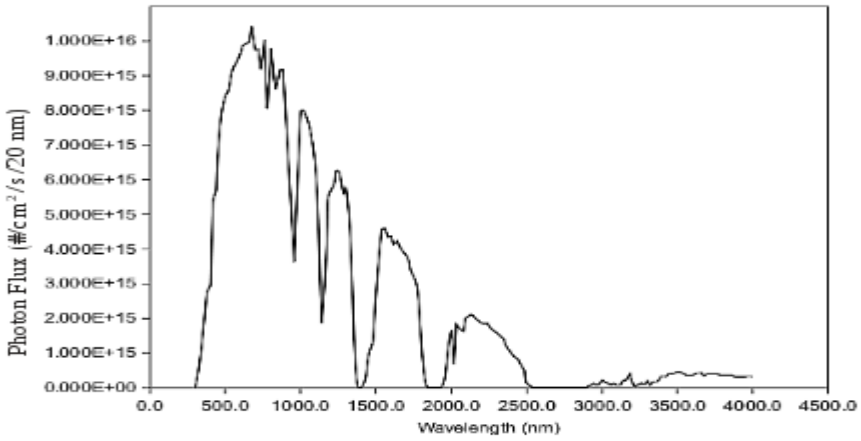

Figure 1.5: Solar energy spectra [Adapted from Fonash S. J.]

In solar cells' energy generation, Photon spectra as depicted in Figure 1.5 are much preferred because in the most desirable way one photon translates to an electron- hole pair for the energy conversion (see Figure 1.6 below).

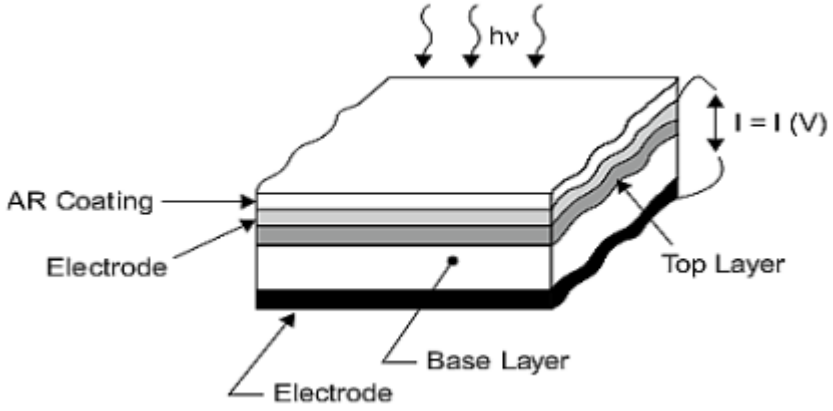

Figure 1.6: Cross-section of a typical solar cell [Adapted from Fonash S. J.]

1.5 Problem Statement/ Hypothesis

Device efficiency and reliability are affected in a drastic manner by the interfaces of the semi-conductor and the electrical contacts. Due to this, the electrical contacts has to be designed in a way as to enable the interfaces exhibit low resistance, low operating voltage and stability to minimize device degradation[10]. Building electronic devices on deformable and flexible substrates is a requirement for novel large-area electronics, such as electronic textiles, electronic paper, sensor skin for robotics or medical prosthesis, and drapable solar cell or flexible displays. Amorphous silicon and silicon nitride, are brittle inorganic semiconductor device materials and as such crack easily when subjected to a significant amount of mechanical strain. The relationship between the optoelectronic performance of the devices and that of the applied mechanical strain values that are below the fracture strains and the strains associated with the loss of device functionality would be analysed to gain understanding in that light.[11] With this knowledge that bending strains affect the optoelectronic and failure mechanisms in bendable substrates, the brittle glass

substrate mostly used in the manufacture of organic electronic devices to would be replaced in this work with a flexible or bendable substrate to attain a highly robust device. From theory, Poly-Dimethyl Siloxane (PDMS) or Polyethylene terephthalate (PET) could both serve as good candidates for this work.

1.6 Scope of Work

The aim of this research is to understand the mechanical behaviour of the manufacture bendable thin film solar cell or photovoltaic. As layers are deposited, the IV and deformation characteristics would be measured. The effects of stress on failure and the I-V characteristics would then be finally modelled and simulated using the Abaqus software to explain the bending effects of the optoelectronic and failure of the manufactured photovoltaic individual layers and the complete structure.

1.7 Arrangement of Work

Chapter one, gives an introduction to the general view of what organic electronics entails particularly focussing on photovoltaic devices. Chapter two theoretically looks at the organic solar cell, the literature review of the work of others on this subject area and how they are related to this work. This chapter also shows how relevant it is to manufacture a plastic substrate organic solar cell other than the more conventional brittle glass substrate. The experimental work on the manufacture of the organic solar cell on the PET substrate and the simulations of the bending tests of the device can be found in chapter three. Chapter four contains results and discussions. The concluding remarks and recommendations for further studies on the effect of bending on the performance of the manufactured organic solar cell can be found in chapter five.

CHAPTER TWO

LITERATURE REVIEW

2.1 Introduction

Thin film photovoltaic initially appeared as small strips powering pocket sized calculators. This technology is now available in very large modules used in vehicle charging systems and very complicated building- integrated installations. Thin film production has been projected by the GBI Research to grow 24% from 2009 levels and to reach 22,214 MW in 2020."Expectations are that in the long-term, thin-film solar PV technology would surpass dominating conventional solar PV technology, thus enabling the long sought-after grid parity objective"[1, 2]. Also organic thin film materials vastly offers an untapped source of possible material properties useful in the semiconductor- based industries. This section delves into the literature work of others beginning from the historical evolution of the organic solar cell to the theoretical background of bendable organic photovoltaic cells.

2.2 Background

Traditional organic materials, in the electronic industry, have been considered as insulating materials [3]. Early work was inspired by photosynthesis in which light is absorbed by chlorophyll, a member of the Porphyrin family [4]. Electro luminescence (EL) response of organic molecular solids was first reported by Bernanose in 1955 [3]. In the 1970's, William et al. developed an organic semiconductor thin film instead of a single crystal semi-conductor films (done earlier by Pope and Helfrich [4, 6]) by vacuum evaporation and longmuir- Blodgett method [7]. However, Tessler et al. were the first to successfully attempt to achieve lasting action from organic semi-conductor materials [8].

Currently, OPVs, OLEDs, organic integrated circuits, radio frequency identification devices, sensors, actuators and memories are various types of organic electronics under extensive investigations to improve their reliability and performance. Many of these low cost applications are the organic semiconductor based devices and as such, their efficiency and reliability needs constant improvements to enable it survive in the market [9]. Silicon solar cell electricity currently makes up over 90% of the photovoltaic (PV) market but its generated electricity is still more expensive compared to that from conventional fossil fuels. This is due to the Single crystal wafers used in the manufacture of solar cells with the intent to increase their efficiency since grain boundaries promote recombination and impede charge transport but the cost of manufacturing these single crystal wafers is very high so the need to look out for an alternative [10].

Depositing organic layers on electrode substrates followed by the deposition of a counter electrode are the basis to the preparation of organic electronic devices. In many instances metals are chosen for the electrodes and these can be doped semi-conductor materials or conductive metal oxides. Stacking various semi-conducting materials on top of each other in the bulk of the solar cell device leads to structures like pn junctions [9].

The deposition methods of these layers vary significantly depending on the materials' system used. Vacuum techniques are used to deposit small conducting organic molecules

whiles printing, spin/ dip coating are used to deposit processed polymer solutions. Finally, thermal evaporation is use to deposit the top electrode layers [9].

2.2.1 The Bulk Heterojunction

The bulk heterojunction organic solar cells will be fabricated on Polyethylene Terephthalate (PET) substrates with Indium Tin Oxide (ITO) anode already deposited on top via sputtering process. Poly-3-Hexylthiophene: [6, 6]-Phenyl-C61-Butyric acid Methyl Ester (P3HT: PCBM) will act as the active layer and Poly (3, 4-Ethylenedioxythiophene) Polystyrenesulfonate (PEDOT: PSS) as the hole injection layer. All the organic layers will be deposited by spin coating whiles the Al cathode will be by vacuum thermal evaporation.

PET is the third most common synthetic polymer and accounts for about 18% of the world's polymer production. PET is aromatic/ aliphatic polyester which possesses very practical thermal properties that are not found in the all aliphatic commodity thermoplastics polyethylene or polypropylene. It has a glass transition temperature near 67°C and a melting temperature of 265°C [11]. PET can exist as an amorphous (transparent) or as a semi- crystalline (opaque and white) thermoplastic material. It generally has a good resistance to mineral oils, solvents and acids with the exception of bases. The semi-crystalline PET has good strength, ductility, stiffness and hardness whiles the amorphous PET has better ductility but less stiffness and hardness [12].

PEDOT has excellent transparency in the visible electromagnetic spectrum region and good electrical conductivity. But even though it is environmentally stable, like most conducting polymers, PEDOT is in-fusible and insoluble making it difficult to process in thin film form. Due to this a water dispersion of PEDOT doped with PSS has become the most promising and most widely used hole injecting material in organic thin film research today. This thin layer of PEDOT:PSS on ITO surface increases the maximum luminance of the device, reduces the threshold voltage by more than 50% and eventually increases the lifetime by the factor of 10 (Pichler 1997,Moliton 2001). Lastly, the PEDOT: PSS acts as a physical barrier against the many defect sites present in the ITO [13].

Since limited absorption spectra and poor charge mobility are the main factors that affect the relatively low efficiency of organic solar cells, combining a narrow- band donor with a fullerene derivative will be an approach to solving this challenge. The most efficient fullerene derivative based donor- acceptor copolymer is P3HT: PCBM blends [14, 15]. PCBM (fullerene derivative) plays the role of electron acceptor in many organic cells due to its high hole mobility tendency. P3HT is from the family of Polythiophene which is a kind of conducting polymer. The photovoltaic effect in the blend is due to the excitation of the p- orbit electron in P3HT [16].

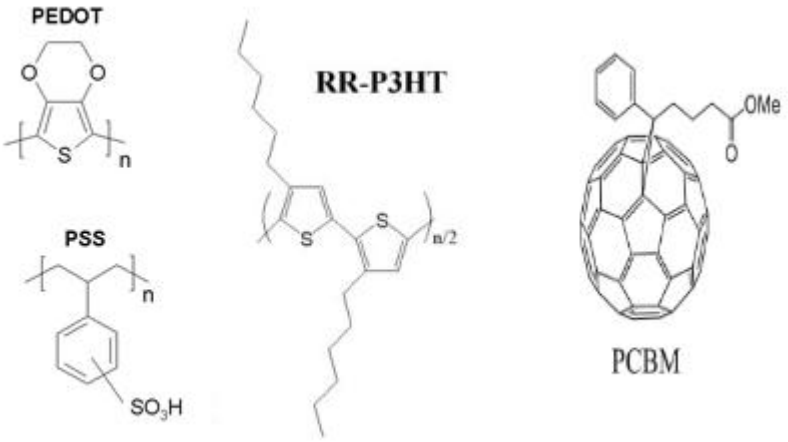

Figure 2.1: Chemical Structures of the Organic layers

Figure 2.1 shows the chemical structures of the various constituents of the organic layer of the photovoltaic cell to be fabricated.

2.3 Plasticity

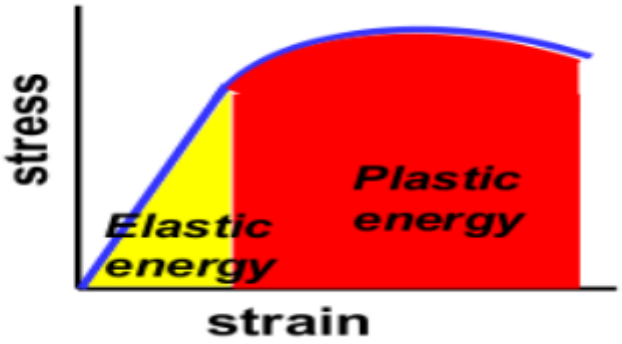

Figure 2.2: Deformation of plastic and elastic relation [Adapted from Tapany Udomphol]

From Figure 2.2 it can be clearly noticed that the plastic deformation does not depend on Hook's law meaning it is a non-reversible process. Plasticity in structural design predicts the maximum load which can be applied to a body without the occurrence of excessive

yielding aside the other aspect that deals with large plastic deformation requirement in changing metals into desired shapes [17].

2.3.1 Plasticity in Solar Cell Manufacturing

Recently, the interest in the use of plastics as substrates for thin solar cells is increasing in order to again cut down on the costs of manufacturing by means of roll to roll deposition, aside the fact that they offer novel possibilities in building integration [18]. In this thesis, PDMS or PET would be chosen as a substrate for the solar cell to be manufactured due to the attractive combination of the former's stretch- ability aside its ease of processing, and the latter's bendability [19].

The lack of the ability of PDMS to measure the angular separation of images that are close together (resolution) when used in intermediate molds propelled this work to use PET as the device substrate. This means that even though PDMS is ultraviolet (UV) transparent, its use in intermediate molds leads to replicas with smooth textures. Smoothing of these master textures has been demonstrated to be beneficial in solar cell application cases. Meanwhile, the detrimental or beneficial effects of replication losses cannot be guessed in general as they depend on the original or pilot textures and device configuration [18].

2.4 The Electrical Interactions at the Organic Solar Cell Interface

Abrupt and cleaner interfaces are allowed when organic semiconductors are deposited on metal.

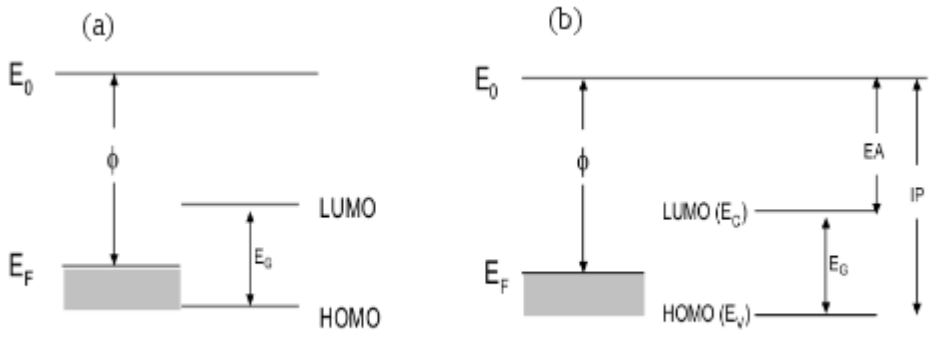

Figure 2.3: Energy level diagram of a metal and semiconductor (a) before contact (c) when contact is made. [Adapted from Korhan Demirkan]

In Figure 2.3 (a), the highest occupied state in the metal is denoted by E_F (Femi level). The minimum energy requirement for an electron to be removed from the surface of the metal to the vacuum level(vacuum of zero kinetic energy) is termed the surface work function (ϕ) whiles E_C and E_V are the valence and conduction band edges respectively [9].

HOMO (Highest Occupied Molecular Orbital) and LUMO (Lowest Unoccupied Molecular Orbital) levels are the names given to energy bands in organic semiconductors since they are not continuous.

The difference between the vacuum level and the conduction band edge (which is a constant of the material) of the semiconductor is termed electron affinity (EA). The band gap E_G is also a constant of the material. The difference between the vacuum level and the valence shell is referred to as the ionization potential (IP). In Figure 2.3 (b), the abrupt discontinuity of allowed energy states at the interface is clear and this forms an energy barrier for charge transport and eventually affects the interface resistance [9].

The closer energy level alignment suggests lower barrier at the interface and higher efficiency for charge injection. The rule for interface engineering is seen in matching the work function of the electrode with the EA and IP of the semiconductor. The Fermi level of a low work function metal aligns more closely with the LUMO level of the semiconductor with the assumption that the chemical potential of the metal and semiconductor do not equilibrate when in contact (as can be seen in Figure 2.4 below). Similarly, a high work function metal's Fermi level will align more closely with the HOMO level of the semiconductor [9].

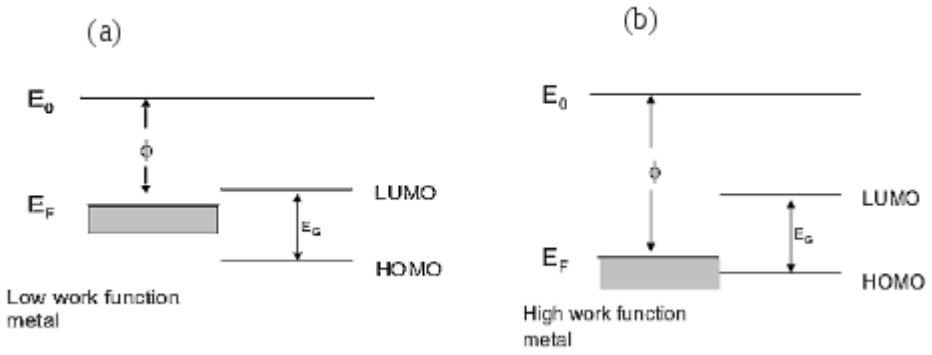

Figure 2.4: Energy offsets (a) Low (b) High [Adapted from Korhan Demirkan]

In an ideal manner, there should be negligible resistance to current flow at the interface of the contact compared to the bulk of the semiconductor. So an essential task for engineering efficient semiconductor device would be to determine the energy states that contribute to the charge transfer since these states at the interface are not always energetically

aligned causing a barrier for the charge transfer process. It should be noted that the charge transport process at the interfaces occurs from the de-localized states of the metal into the localized states of the organic semiconductor.

With adequate design, negligible resistance to current flow can be achieved at the metal/ semiconductor interfaces. For inorganic semiconductors, heavily local doping will provide tunneling or Ohmic contacts whiles it is not always viable for organic semiconductors. Organic semiconductor doping is an interstitial process, a substitution for inorganic crystalline semiconductors [9].

2.5 Theory

The challenging aspect of flexible substrates in solar cell manufacturing is the extent to which it can be deformed. Letting a pair of couple of magnitude M (Moment) be applied to the ends of the substrate as shown in figure 2.4. It is clear that the longitudinal filament of which this beam-like substrate may be thought to be composed will be contracted on the face of the beam toward the centre of curvature, and those on the opposite of face will be extended. The central line is the name given to the line passing through the centroids of the flexible substrate [20].

The terminal coupling of this substrate of length, L with a central line length, L_o after bending (as shown in figure 2.5) defines an engineering strain given in equation 2.0.

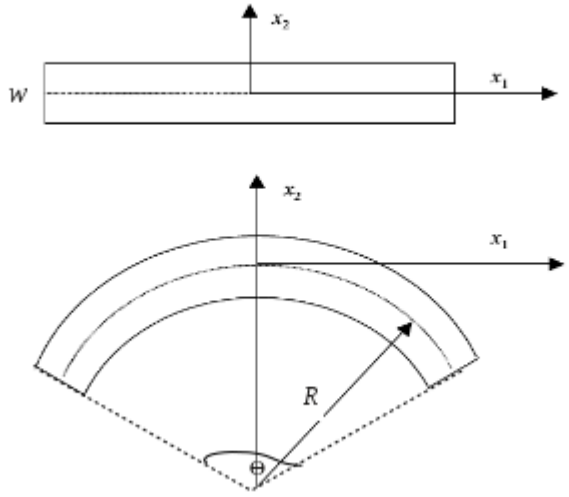

Figure 2.5: The schematics of a bendable organic photovoltaic single layer of width, w and a radius of curvature, R

From Figure 2.5, if the assumption is that the central line indicated by a dotted curve is unaltered in length and its plane sections normal to the central line also assumed to remain plane and normal to the deformed central line [20], it is easy to detect that the strain (the magnitude of the extension or contraction) is:

$$\text{Strain, } \varepsilon = \frac{l - l_o}{l_o} = \frac{\left(\mathrm{R}+\frac{w}{2}\right)\theta - \mathrm{R}\theta}{\mathrm{R}\theta} = \frac{w}{2\mathrm{R}} \qquad (2.0)$$

Where ε above represents the engineering strain whiles the true strain, ε_T is given as:

$$\varepsilon_T = \int_{l_o}^{l} \frac{dl}{l} = \ln\left(\frac{l}{l_o}\right) \qquad (2.1)[21]$$

From literature these two are related by the graph shown in Figure 2.6.

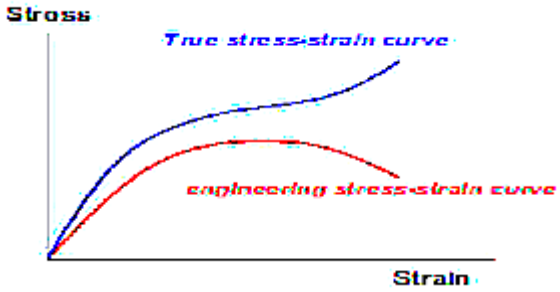

Figure 2.6: Relationship between true and engineering stress-strain curves (Adapted from Tapany Udomphol [17])

This therefore implies that the true stress is the load divided by the instantaneous area so it can represent the true deformation characteristics of the material unlike the engineering stress and strain curve in figure 2.6.

If the distance from the central line to the surface of the substrate is

$$\frac{w}{2}=y \qquad (2.2)$$

Then the strain becomes;

$$\varepsilon=\frac{y}{R} \qquad (2.3)$$

Clearly, the strain is directly proportional to y, meaning that the smaller the substrate thickness the lower the strain. This result is very desirable since we seek to manufacture a solar cell of very low strain when bent. Relating these results to the stress,

$$\sigma = E\varepsilon = \frac{Ey}{R} \qquad (2.4)$$

means that the deformation of the manufactured solar cell could be studied. This implies that;

$$\frac{\sigma}{y} = \frac{E}{R} = \frac{M}{I} \qquad (2.5)$$

Where; E is the Young's modulus, R the radius of curvature, M the moment and I the moment of inertia. See Appendix for the complete derivation of Equation 2.5 from 2.0.

2.6 The Bending Theory

These assumptions below are made in order to develop the elastic theory of the thin film bending.

1. The thin film has a constant, prismatic cross-section and is constructed of a flexible, homogenous material that has the same modulus of elasticity in both tension and compression (shortens or elongates equally for same stress).
2. The thin film material is linearly elastic; the relationship between the stress and strain is directly proportional.
3. The thin film material is not stressed past its proportional limit.
4. A plane section within the thin film before bending remains a plane after bending (see below AB & CD in Figure 2.7).

The neutral plane of the thin film is a plane whose length is unchanged by the beam's deformation and this plane passes through the centroid of the cross-section [22].

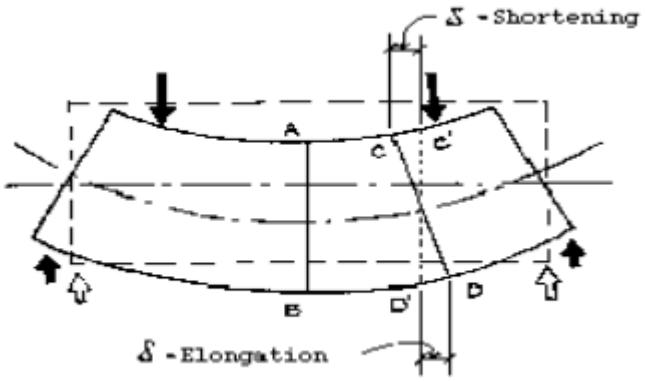

Figure 2.7: The process of bending [22]

The thin film is represented in Figure 2.7 by dashed lines and the neutral axis and lines AB and CD are drawn parallel to their respective sides. Lines AB and C D are separated by some distance as can be clearly notice in the diagram above. These two lines were parallel before bending and due to the assumptions above, the thin film is expected to behave as a beam undergoing bending, meaning these lines would remain perpendicular to the neutral axis [22].

Figure 2.8 depicts a typical stress–strain curve obtained polymers.

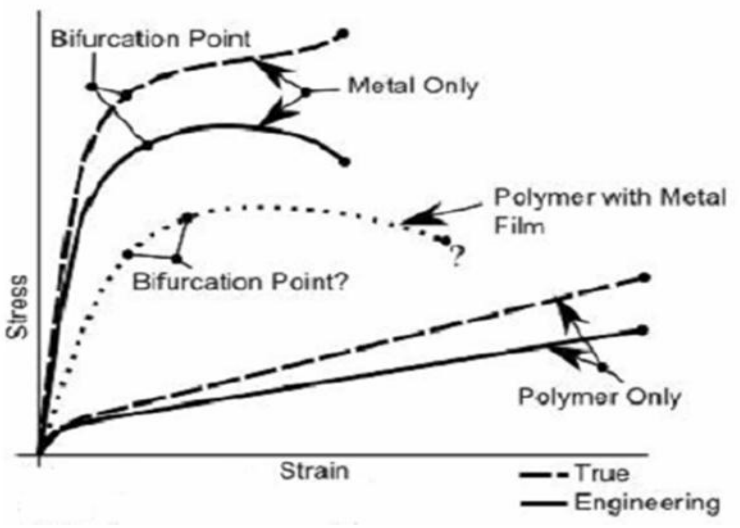

Figure 2.8: Stress- strain curves for polymers

Bending also known as flexure characterizes the behaviour of a slender structural element subjected to an external force applied to an axis of the element perpendicularly. A beam is any element whose length is considerably larger than the width and the thickness [24].

2.6.1 Technique One (3 Point Bend Test)

The first technique to be discussed is the three point flexure technique. This flexural test measures the force required to bend a beam under three point loading condition [24]. The three point bending flexural test provides values for the modulus of elasticity in bending, flexural stress, flexural strain and the flexural stress- strain response of the material. Ease of the specimen preparation and testing is the main advantages a three point flexural test. Result sensitivity to the specimen type, loading geometry and the strain rate are the disadvantages of this method. For rectangular cross section such as in thin films (the one employed in this research) the flexural stress, σ_f and strain, ε_f are given by

$$\sigma_f = \frac{3PL}{2bd^2} \qquad (2.6)[25]$$

$$\varepsilon_f = \frac{6Dd}{L^2} \qquad (2.7)[25]$$

Where L is the support span in mm, P is the Load or force at a given point on the load deflection curve in N, b is width of test beam in mm, d is the depth of tested beam, and D is maximum deflection of the centre of the beam in mm.

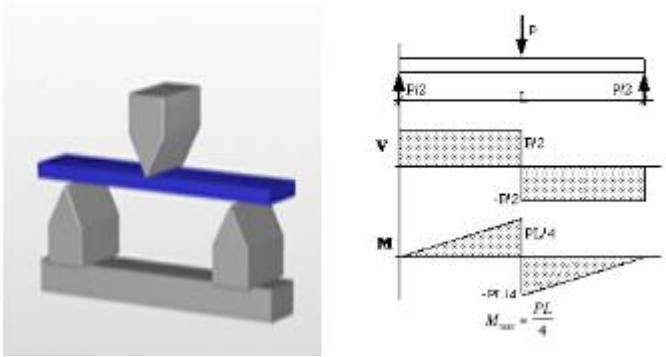

Figure 2.9: Three point flexure test set-up and graphs

Finally, the flexural modulus of the test element can also be calculated using the formula below;

$$E_f = \frac{L^3 m}{4bd^3} \qquad (2.8)[28]$$

Where m is the gradient of the initial straight line portion of the load deflection curve in N/m and E_f is the Flexural modulus of elasticity in MPa.

2.6.1.1 Plastic bending

The Euler Bernoulli equation, = My/I, is valid only when the stress at the extreme fiber (which is the portion of the test element farthest from the neutral axis) is below the yield stress of the material from which it is constructed. The stress distribution becomes non-linear at higher loadings and if it is a ductile material, it will eventually enter the plastic hinge state (see Figure 2.1) where the magnitude of the stress is equal to the yield stress everywhere in the test element where the stress changes from tensile to compressive [25].

2.6.2 Technique Two (4 Point Bend Test)

Four point bending is used to measure effectively the bond strength of the test element. A uniform maximum moment and an area of tension at the bottom of the specimen is achieved in this bending technique [29]. Figure 2.10 depicts the set- up and the estimated graphs that can be gotten from this four point flexural test.

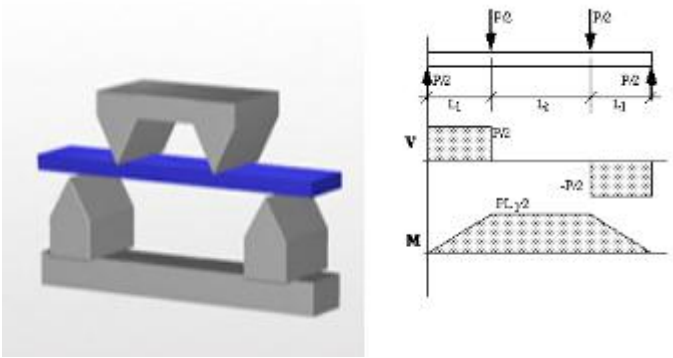

Figure 2.10: 4 point bend test setup and graphs [26, 27]

2.7 The efficiency of a conventional photovoltaic cell

The optical transitions across the band gap generate the current produced by solar cells. Direct transitions where the momentum of the resulting electron-hole pair is very close to

zero, and indirect transitions where the resulting electron hole pair has a finite momentum are the two distinguishable types of optical transitions whereby the latter transition requires the assistance of a quantum of lattice vibration (also called phonon) [30].

The performance of photovoltaic devices are characterized by the short circuit current (J_{SC}), the open circuit voltage (V_{OC}), and the fill factor (ff) via Figure 2.11 which depicts the current- voltage curve of a photo-diode under illumination.

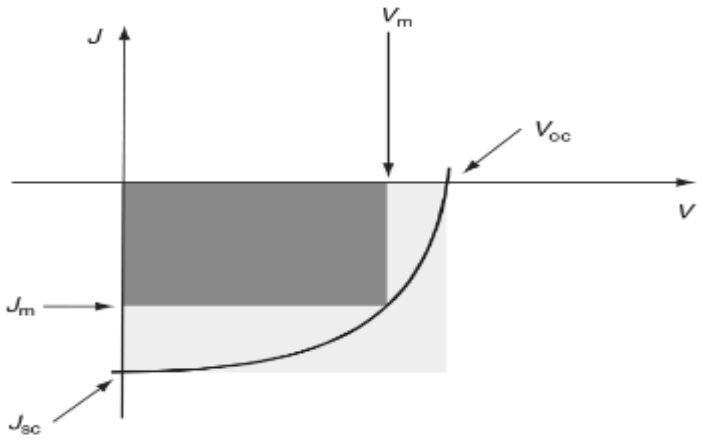

Figure 2.7: Current- Voltage spectra of a photovoltaic under illumination [adapted from Paul A. Lane et al.]

From Figure 2.11, the fill factor of the illuminated photovoltaic device can be calculated by using Equation 2.6.

$$ff = \frac{P_m}{I_{SC}V_{OC}} = \frac{I_m V_m}{I_{SC}V_{OC}} \qquad (2.6)\ [31]$$

Where P_m is the maximum power delivered to an external circuit and the product of I_{SC} and V_{OC} represent the potential power of the device.

The Power conversion efficiency, η_e of a device will therefore be given as η_e.

$$\eta_e = \frac{P_m}{P_o} = \frac{I_m V_m}{P_o} \qquad (2.7)\ [31]$$

Where Po is the incident optical power. Therefore the spectral response of OPVs is an important way to characterize such devices to optimize their performance.

The external quantum efficiency (also called the Incident Photon conversion efficiency), EQE is given by the number of electrons generated per incident photon:

$$EQE = \frac{\eta_e}{\eta_{ph}} = \frac{I_{SC} hc}{P_o \lambda e} \qquad (2.8)\ [31]$$

Where λ is the wavelength of light, e is the electrical charge, h is Planck's constant, and c is the speed of light. This generally follows the absorption spectrum of the materials constituting the OPV. The internal quantum efficiency, IQE also known as the photo current action spectrum has the relation:

$$IQE = \frac{PhotoCurrent}{AbsorbedPhotonFlux} \quad (2.9)\ [31]$$

The performance of a bilayer OPV is ultimately determined by the efficiency of charge photo generated and charge transport. As charge transfer takes place at organic hetero-junction (Figure 2.12) absorption must take place at the interface or within the exciton diffusion length in the respective materials [31, 32].

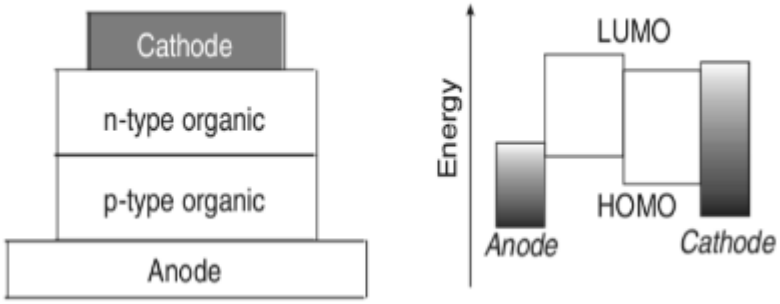

Figure 2.8: The schematic diagram of a heterojunction OPV [adapted from Paul A. Lane et al.]

One primary limitation of a heterojunction solar cell is that charge photo-generation occurs only in a thin layer near the organic heterojunction. Here, only a fraction of incident light will be absorbed in this region, limiting the quantum efficiency of devices. Co-evaporating two organic pigments to create a bulk heterojunction is one way of increasing the width of the photocarrier generation region [33].

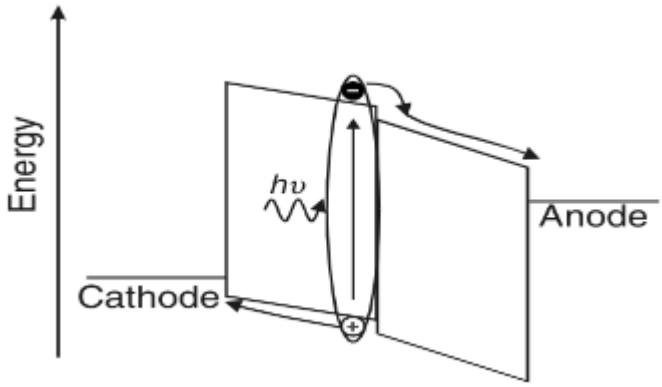

Figure 2.9: Photo-induced charge transport illustration [adapted from Sam-Shajing Sun et al.]

Figure 2.13 shows that electrons and holes are photo-generated in the mixed layer and are swept to the transport layers by this built in chemical and electrical potentials [34, 35].

CHAPTER THREE

EXPERIMENTAL PROCEDURE/ MODELING

3.1 Introduction

This section contains the experimental and the modeling parts of this research. Experimentally, the organic photovoltaic cell will be fabricated layer by layer alongside characterising the thin film layers deposited at each stage.

3.2 Experimental Work

The experimental part has been classified into four sections; mask designing, sample preparation, deposition, and the three point bend testing of the deposited layers. Since the PET was obtained with ITO already deposited on it, the mask to be designed was done for only the Aluminium cathode.

3.2.1 Dimensions of the Solar Cell

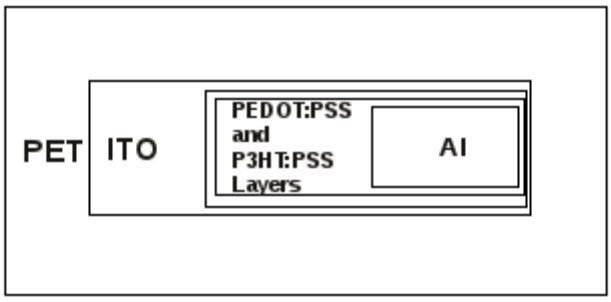

Figure 10.1: Top view of the complete bendable Solar Cell to be manufactured

A mask was designed for the Aluminium (Al) cathode (as indicated in Figure 3.1) deposition with 0.75x0.75 cm^2 dimensions.

3.2.2 Sample Preparation and Cleaning

The flexible substrate, Polyethylene terephthalate (PET), used was not synthesised but obtained from the company called SOLARONIX (www.solaronix.com). The PET had ITO already deposited on it (product name: PETITO 175-60). 75x25 mm^2 and 25x25 mm^2 ITO/PET substrates were cleaned in Iso-propyl alcohol (IPA) and dried in a stream of nitrogen gas (N_2). This process involved immersing in ethanol for five minutes, rinsing with deionised water and placing in IPA (Iso Propyl Acid). The IPA with the samples in a glass beaker was placed into an ultrasonic water (Figure 3.2) bath for about 5 minutes at room temperature (30 degrees Celsius) followed by the Nitrogen gas drying.

Figure 3.11: Ultrasonic water bath

3.2.3 Solar Cell Manufacturing Procedure

The organic solar cell to be fabricated (see Figure 3.3) uses Poly-3-hexylthiophene: [6, 6]-phenyl-C61-butyric acid methyl ester (P3HT: PCBM) as the active layer and Poly (3, 4-ethylenedioxythiophene) polystyrenesulfonate (PEDOT: PSS) as the hole injection layer.

These organic layers were deposited by spin coating while the Al cathode by vacuum thermal evaporation.

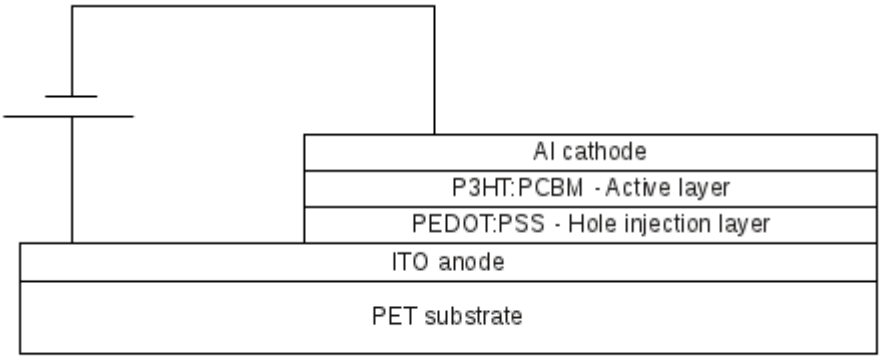

Figure 12: Bendable solar cell side view

3.2.3.1 Spin coating of Organic Layer

The hole injection layer (PEDOT: PSS) and the blend or active layer (P3HT: PCBM) were deposited by spin coating with the WS- 650Hz- 23NPP/ A3/ AR2 spin coater model using the parameters below.

Table 1: Spin coating parameters for organic layers

Parameters	PEDOT:PSS		P3HT:PCBM	
Steps	1	2	1	2
Time/ s	10	40	10	30
Speed/ rpm	500	2000	400	800

Figure 13.4: The Spin Coater

In preparing the blend for spin coating, a 1:1 weight ratio of P3HT: PCBM was employed. 25.86mg and 24.12mg of P3HT and PCBM were dissolved in a 5ml volume of Chloro-benzene via stirring for 12 hours. See Appendix for details in calculating the blend weight composition.

3.2.3.2 Thermal Evaporation of Cathode Layer

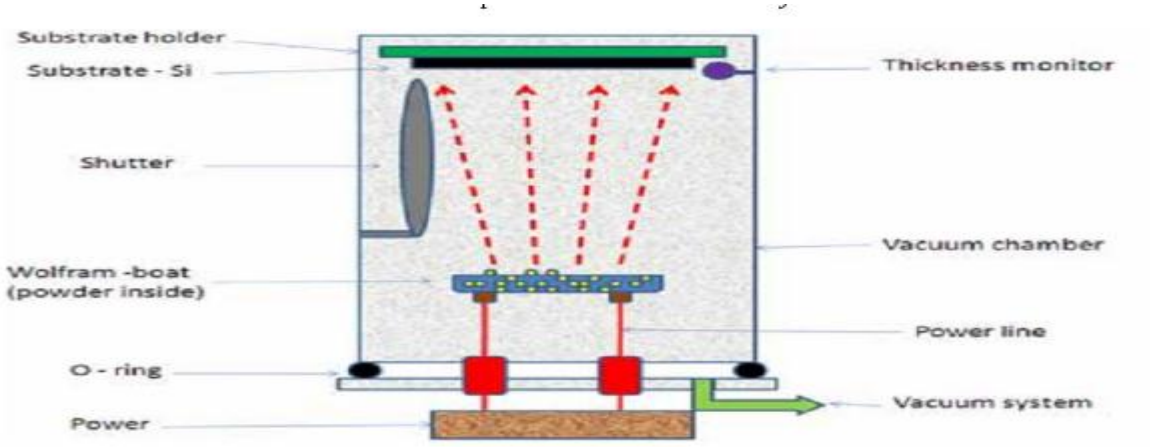

Figure 14: Schematic diagram of thermal evaporator

The Al cathode was evaporated in an Edward Auto 306 coater at room temperature. The final device configuration was Al / P3HT: PCBM/ PEDOT: PSS/ ITO/ PET with a device area of (0.75x0.75) cm^2.

3.3.4 Characterization of Bendable OPV Device and Layers

The ITO thickness of 1055 Å, as confirmed by the optical simulation of its Transmittance (See Figure 3), measured and the surface roughness of each layer was carried out using the Dektek 150 Surface Profiler. The optical transmittance, T was also measured for the various layers using an Avouts UV-VIS spectrophotometer. 3 point flexure test measurements were taken on the various device layers using the TIRA test 2810 machine. The light and dark I-V were measured using Keithley 2400 Source Measure Unit (SMU) under An1.5 illumination making use of an Oriel Class A solar simulator.

3.3.5 TIRA Test

The first element used to undergo the 3 point bend test had the dimensions of 75x25 cm^2. Figures 3.5, 3.7 and 3.8 shows the flexural processes during the TIRA test.

Figure 15: ITO/PET element in un-deformed state

Figure 16: ITO/PET element in deformed state

Figure 17: ITO/PET element returns to original state

Form Figure 3.7 and 3.8, it can be concluded that the elastic limit was not exceeded meaning the flexure was elastic.

The tensile strengths (for both compressive and tensile bending of ITO on PET) were calculated and the stress and strain curves were plotted using the force against displacement plot extracted from the test results. This test was repeated for subsequent deposition of the organic layers. The only difference is that, the element size/ dimension was reduced to $25x25cm^2$ due to the element requirement for spin coating.

3.4 Modeling and Simulation

This modelling section began with simulating the unknown thickness of ITO on the PET substrate obtained from SOLARONIX (Sample name: PETITO 175-60). Matlab was used to simulate the bending moments and Abaqus was used to model the displacement behaviour of the 3 point flexure test.

3.4.1 "Optical" Modeling

Since ITO was already deposited on the PET substrate (PETITO 175-60) obtained from SOLARONIX (www.solaronix.com) without the specification of its thickness on the 175 micrometres thick PET the "optical" software alongside the transmittance data of the ITO/PET was used to simulate and confirm the thickness of ITO.

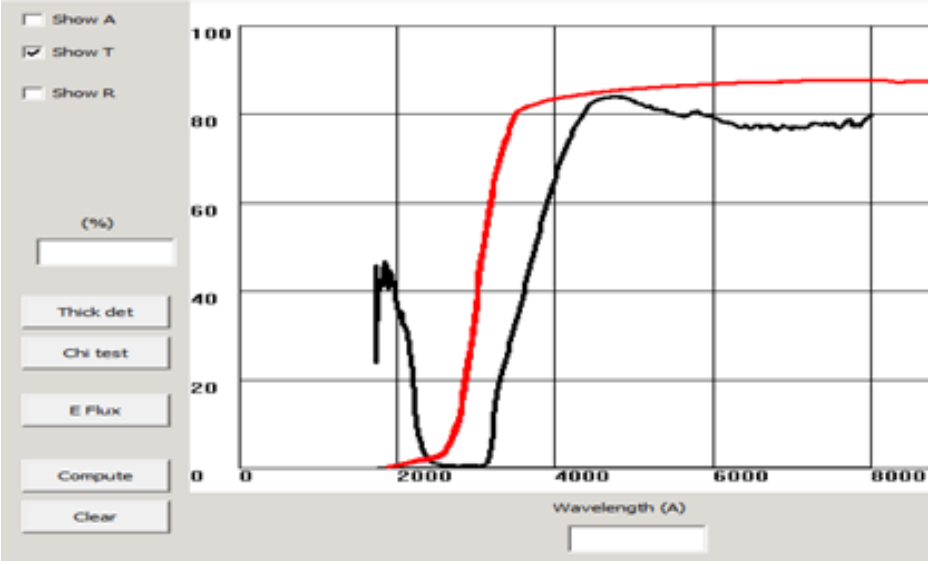

Figure 18: "Optical" software reticule displaying both theoretical and experimental transmittance data of ITO/PET

The Physics behind this mechanism is that the experimental data is compared with theoretically defined layers using their refractive index and extinction coefficient.

3.3.2 Matlab Modeling

The Matlab programme was used to determine the bending moments of the ITO layer. Here, the nodal and elemental sections where defined using the K and J metrices and material properties to model the 3 point bending in the un deformed and deformed forms. The reaction forces were also modeled which eventually gave values for the bending moments being of the individual thin film layer defined.

3.3.3 Abaqus Modeling

The Abaqus/ CAE student edition 6.9-2 creates models for analysis and interpretation. The modeling of the 3point flexure test began with the step of creating the parts as a 3D deformable shell planar, with dimensions corresponding to the physical specimen. The material is defined by inputting its properties which included its Poisson's ratio and

Young's Modulus. The support effects were modeled using constraints by partitioning the plane to generate 3 nodal sets. This approach was used instead defining analytical rigid rollers or supports because the latter proved to be difficult. The boundary conditions used at these three nodes depicted the 3 point bend rollers (see Figure 3.6)

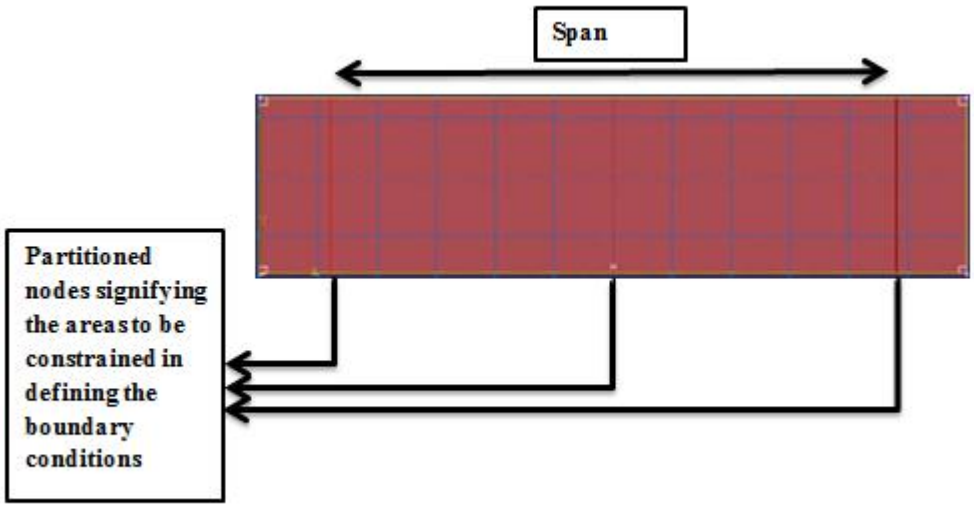

Figure 19: Partitioned nodes to define the 3 point bend part

The model is instanced as a dependant mesh followed by meshing all the four sections created due to the 3 partitions. Also, the sections were defined to have structured quad element. The boundary conditions set at the nodal points included fixing the support sections in the Z and X direction (i.e. U2 and U3). The middle roller set defined by the partitioned middle line was set to displace downward (i.e. move only in the U3 direction).

Figure 3.11 depicts the deformed and that of the un-deformed 3 point bend contour models.

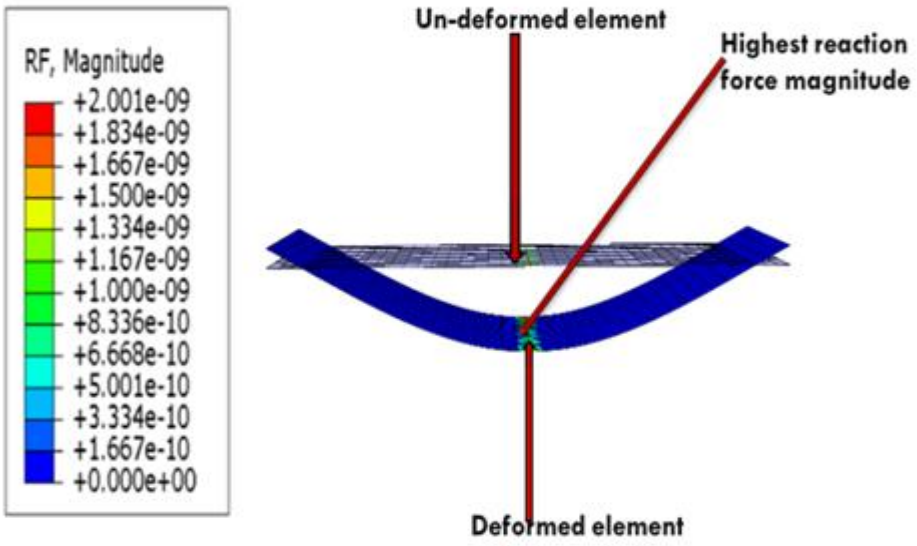

Figure 20.11: The 3 point model parts and results obtained from the Abaqus/CAE.

CHAPTER FOUR

RESULTS AND DISCUSSION

4.1 Introduction

Plastic deformation (depends on the loading path by which the final state is achieved) is not a reversible process like elastic deformation (which depends only on the initial and final states of strain) [1].

4.2 Results and Discussion

The simulation and optimization of the optical transmittance of the ITO/PET multilayer system along with their experimental data on the "Optical" Software provided an average value of 1055 Armstrong for the thickness of the ITO layer on the PET substrate. Moreover, the results obtained from the Abaqus/CAE modeling showed that at the middle of the deformed thin film layer, the occurrence of cracking was very susceptible since that section experiences the highest reaction force magnitude. The roughness of ITO on PET was determined from Profilometry to be 33.8 Armstrong whiles that of PEDOT: PSS/ ITO/ PET gave an improved roughness of 15.4 Armstrong. Resistivity of the TCO (ITO) was 60 ohms/sq. before bending and the results on bending have been summarized in Table 2.

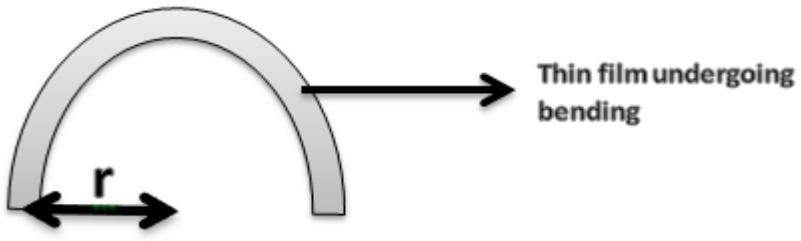

Figure 21.1: Schematic diagram of a thin film undergoing bending

Table 2: Electrical conductivity of ITO/PET

Curvature Radius/ mm	Average Resistivity/ ohms per square
∞	60.000
30	68.172
25	46400.000
20	96400.000

The ITO anode and hole injection layer (PEDOT: PSS) exhibited 80- 85% transmittance in the UV- VIS Spectrum in Figure 5. From this Figure, it is clear that bending has very minimal effect on their transmittance.

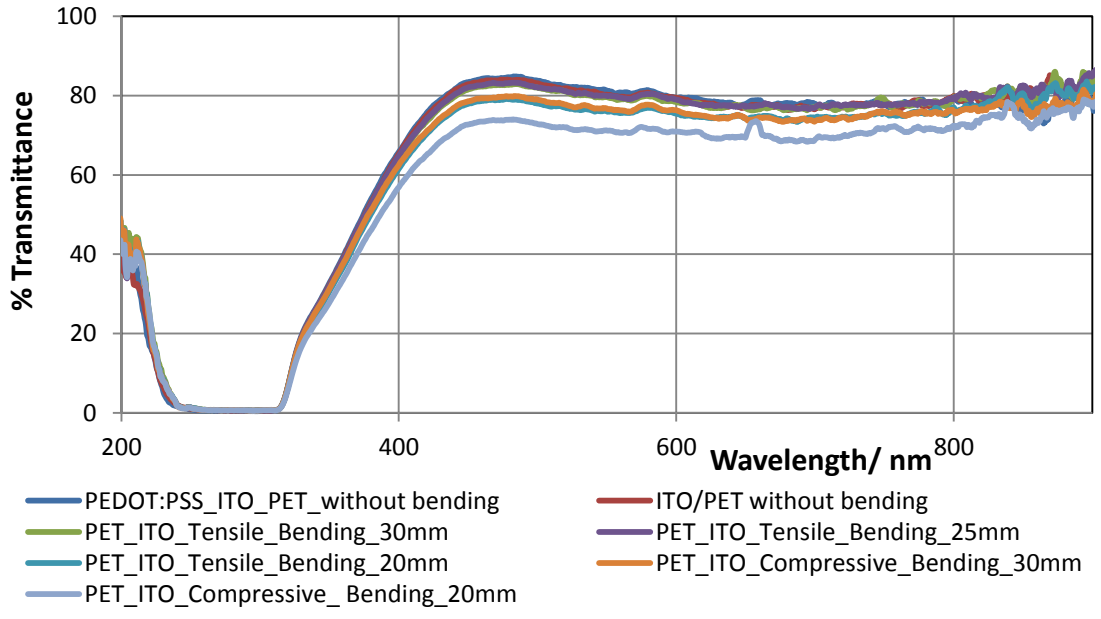

Figure 22: Minimal variation in transmittance during bending of ITO on PET

It is also clear that as the bending increased, the strain increased alongside with the cracks causing part of the incident light undergoing transmission to be absorbed. This therefore indicates that the higher the strain, the more susceptible the layers are to absorbing the light to be transmitted.

Even though the SEM results of ITO on PET predicts ITO fragility as seen in Figure 4.3, the bending test (both tensile and compressive) done on it gave very promising tensile strengths, β (β increased from 28.4 to 31.7MPa respectively) as seen in Figures 4.4. The subsequent deposition of layers further increased their β (See Table 3). It is clear from Figure 4.5 that the OPV device fabricated is both strong and tough with reference to the "Mechanics of Polymers" [9, 10] in Figure 4.6. The flexural modulus of the Fabricated OPV compositions was also calculated and the results tabulated in Table 4.

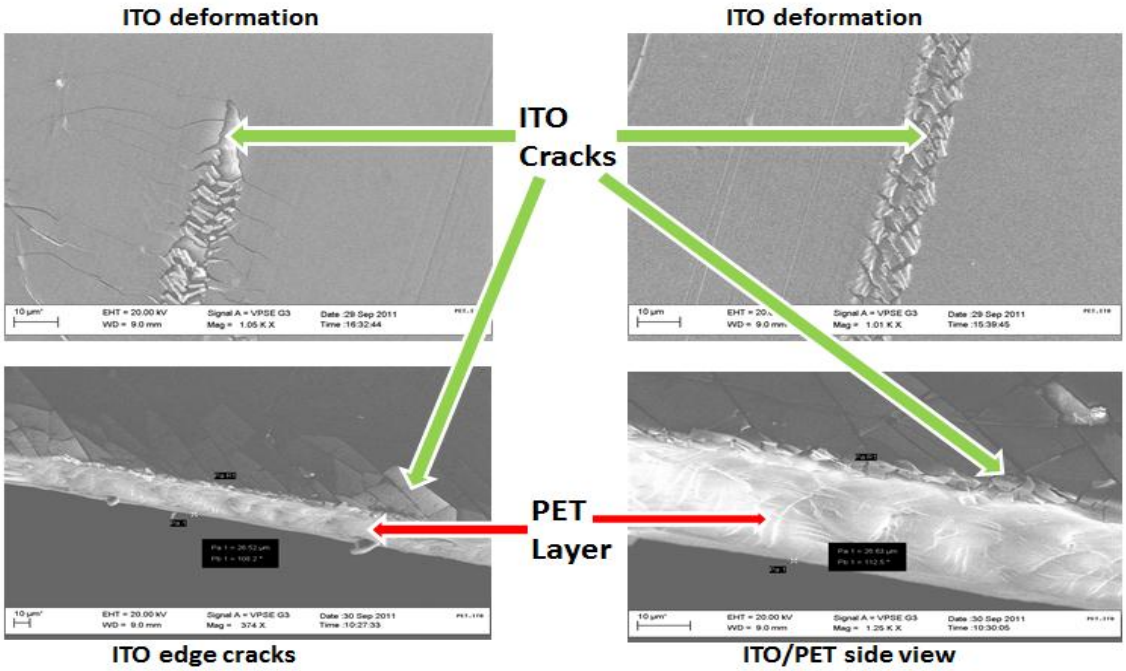

Figure 23: Scanning Electron Microscopy of ITO on PET

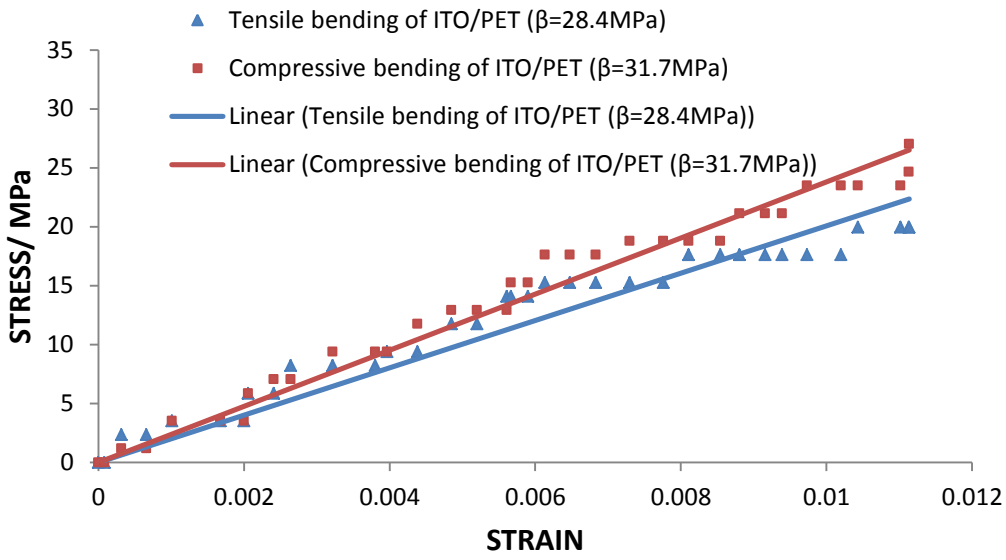

Figure 24: Compressive and tensile bending comparison in terms of β

Table 3: Tensile Strength Variations

Thin Film Layer Composition	Tensile strength, β/ MPa
Al/ P3HT:PCBM/ PEDOT:PSS/ ITO/ PET (Bendable OPV Cell)	51.99
P3HT:PCBM/ PEDOT:PSS/ ITO/ PET	58.75
PEDOT:PSS/ ITO/ PET	53.68
ITO/ PET	28.40

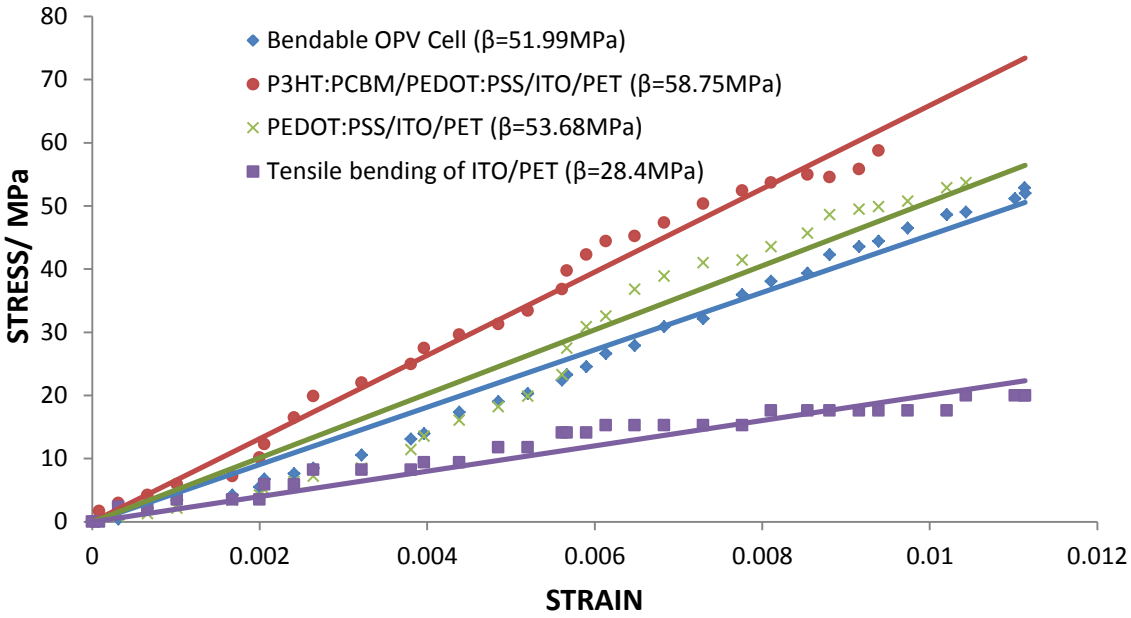

Figure 25: TIRA test results of the OPV layers and device (stress against strain curves)

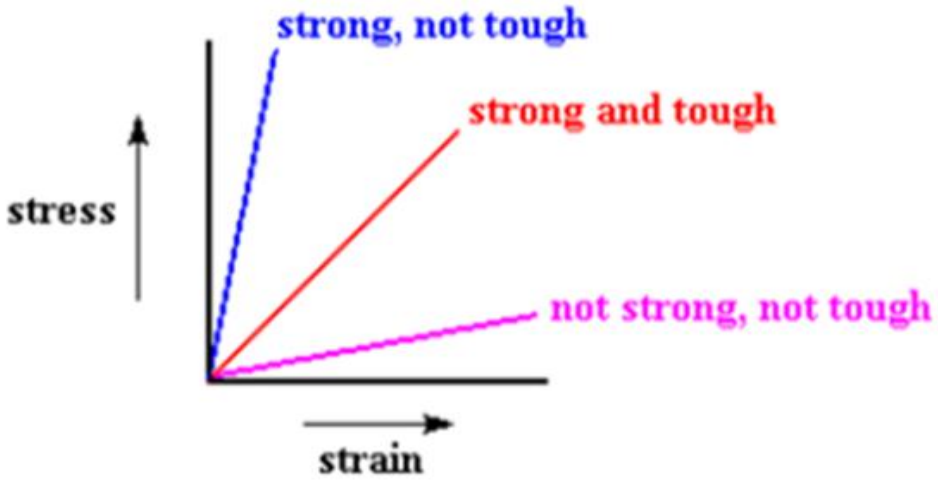

Figure 26: "The Mechanics of Polymers" [2, 3]

Table 4: Flexural modulus of OPV

Thin Film Layer Composition	Force against Displacement Initial Gradient in N/mm	Flexural Modulus in MPa
Al/ P3HT:PCBM/ PEDOT:PSS/ ITO/ PET (Bendable OPV Cell)	0.1714	3217.16
P3HT:PCBM/ PEDOT:PSS/ ITO/ PET	0.1182	2218.602
PEDOT:PSS/ ITO/ PET	0.101	1895.76
ITO/ PET	0.022	412.9377

Finally, the characteristics of the OPV device fabricated behaved like a good diode in the dark as expected (See Figure 4.7). Moreover, its lifespan performance was very desirable in the dark. However IV results obtained from its illuminated state gave a low fill factor value.

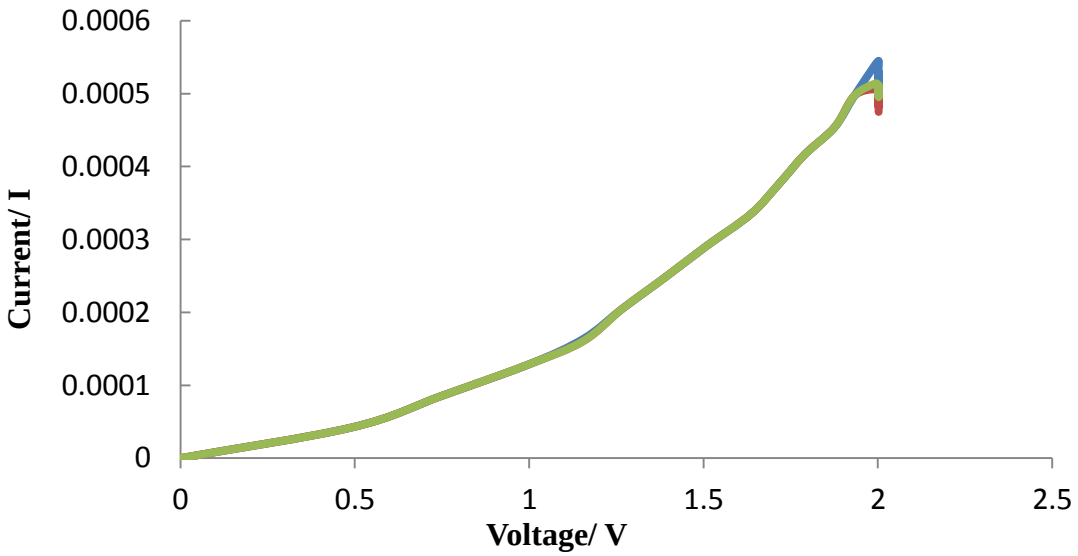

Figure 27: Device Characteristics in the dark

CHAPTER FIVE

CONCLUSION AND RECOMMENDATION

5.1 Conclusion

The bendable Organic Photovoltaic fabricated in this research was found to be strong and tough and the bending effect on transmittance was very minimal (See Figure 9 for the OPV fabricated). The resistivity of the ITO/PET (TCO) increases with cracking and the fill factor was low indicating the need for device optimization.

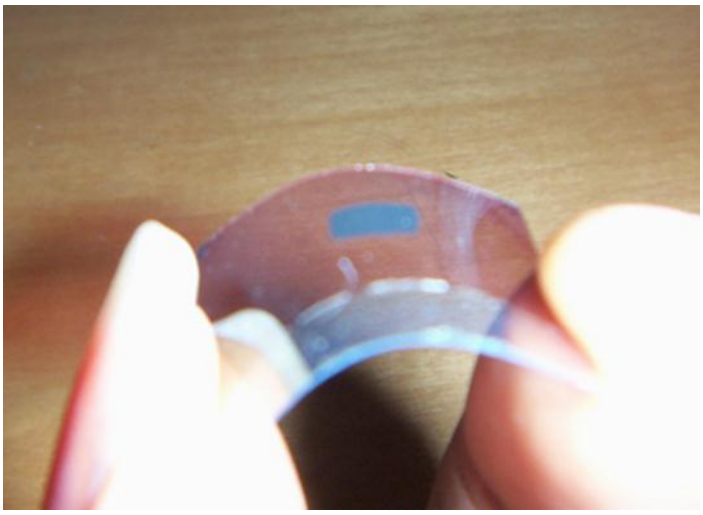

Figure 28: Bendable Solar Cell (OPV) fabricated

5.2 Recommendation

Since the fill factor value obtained from the bendable OPV in its illuminated state was low, the need for device optimization in the future is recommended.

APPENDIX

- PROOF of the Eulerian formula:

$$dF = \sigma dA$$

$$\sum F_x \Rightarrow \int \sigma dA = 0$$

$$\sum M \Rightarrow \int y\sigma dA = M$$

$$M = \int y\left(\frac{Ey}{R}\right) dA$$

$$M = \frac{E}{R}\int y^2\, dA$$

$$where\ I = \int y^2\, dA: second\ moment\ of\ area\ or\ moment\ of\ inertia$$

$$M = \frac{EI}{R}$$

$$and\ since\ \sigma = \frac{Ey}{R} \Rightarrow yM = \frac{Ey}{R}I$$

$$y\frac{M}{I} = \sigma$$

$$\frac{\sigma}{y} = \frac{E}{R} = \frac{M}{I}$$

- Composite of blend calculation:

$$Volume\ of\ chlorobenzene = 5ml$$

$$Density\ of\ Chlorobenzene, \rho = \frac{m}{V} = \frac{1.11g}{cm^3} = 1.11g/ml$$

$$m = \rho V = \frac{1.11g}{ml} \times 5ml$$

$$m = 5.55g$$

$$\Rightarrow Total\ mass\ of\ P3HT{:}\ PCBM + Chlorobenzene = 5.60g$$

$$\therefore Mass\ of\ P3HT{:}\ PCBM = 50mg$$

$$with\ ratio\ 1{:}\ 1$$

$$\Rightarrow Mass\ of\ P3HT = 25mg$$

$$and\ mass\ of\ PCBM = 25mg$$

REFERENCE

Chapter 1

[1] Joseph J. Berry, "Electronics, Photonics and Magnetic Materials", Lecture notes, National Renewable Energy Laboratory (NREL), (May 2011).

[2] http://www.californiascientific.com/resource/solar%20cell.pdf

[3] http://en.wikipedia.org/wiki/Thin-film-solar-cell

[4] T. Tong, B. Babatope, S. Admassie, J. Meng, O. Akwogu, W. Akande, and W. O. Soboyejo, "Adhesion in organic electronic structures", JOURNAL OF APPLIED PHYSICS 106, 083708, American Institute of Physics, pp1-7,(2009)

[5] Hong Ma, et al, "Interface Engineering for Electronics", Advance Functional Materials, WILEY- VCH Verleg GmbH & Co. KgaA, Weinheim, pp: 1- 15,(2010)

[6] G. Harsanyi, "Polymer films in sensor applications", Technomic Publishing Co., Lancastev, Basel, (1994).

[7] http://www.renewableenergyfocususa.com/view/14419/konarka-opv-solar-cell-reaches-83-efficiency/

[8] U.S. Department of Energy, "DOE Fundamentals Handbook- Electrical Science ", Volume 1 of 4, Washington, D.C. 20585, USA, DOE-HDBK-1011, pp:1-92, (June 1992).

[9] Fonash S. J., "Solar Cell Device Physics", Second Edition, Elsevier Inc., pp: 1-5, (2010)

[10] Korhan Demirkan, "Interfaces of Electrical Contact in Organic Semi-conductor Devices", University of Delaware, UMI No.: 3320996, pp 1- 10, (2008).

[11] Akogwu O. E., "Deformation and failure mechanisms in flexible and organic electronic structures", Princeton University, publication number: 3411017, Abstract, (2010).

Chapter 2

[1] http://www.renewableenergymagazine.com/

[2] GBI Research(2011), "Thin Film Photovoltaic (PV) Cells Market Analysis to 2020CIGS Copper Indium Gallium Diselenide to Emerge as the Major Technology by 2020", gbiresearch.com, Retrieved 29 January 2011.

[3] A. Bernanose, "Electro luminescence of organic compound", British Journal of Applied Physics, vol 6, pp: 854- 855, (1955).

[4] Chamberlain, G. A. "Organic solar cells — a review." Sol. Cells, 8(1), pp: 47–83, (1983)

[5] M. Pope, H. Kallmann, P. Magnante, "Electroluminescence in organic crystals", Journal of Chemical Physics, Vol. 38, pp: 2042- 2043, (1963).

[6] W. Helfrich, and W. G. Schneider, "Recombination in anthracene crystals", Physical Review Letter, Vol. 14, pp: 229- 231, (1965).

[7] Roberts G., Ed. "Langmir- Blodgett films", Plenum Press, New York, (1990).

[8] N. Tessler, G. J. Denton, R. H. Friend, "Lasing from conjugated- polymer micro cavities", Nature, Vol. 382, pp: 695- 697, (1996).

[9] Korhan Demirkan, "Interfaces of Electrical Contact in Organic Semi-conductor Devices", University of Delaware, UMI No.: 3320996, pp: 1- 10, (2008).

[10] Peters C. H., et al, "Energy Transfer in Nanowire Solar Cells with Photo- Harvesting Shells", Department Materials Science and Engineering, Journal of Applied Physics 105, USA, (2009).

[11] Robert H Olley, "You're Not Sustainable, PET", October 13th 2010 10:15am, Science 2.0, Join the revolution.

[12] "Material-PET (polyethylene terephthalate)" © 1996-2003 Torben Lenau

[13] https://workspace.imperial.ac.uk/experimentalsolidstate/public/Cleanroom/020-PEDOT-PSS %20Deposition_200609.pdf

[14] Perzon, E.; Wang, X.; Zhang, F.; Mammo, W.; Delgado, J.L.; Cruz, P.; Inganäs, O.; Langa, F.; Andersson, M.R. "Design, Synthesis and Properties of Low Band Gap Polyfluorenes for Photovoltaic Devices". Synthetic Metals 154 (2005) pp.53-56

[15] Al-lbrahim, M.; Ambacher, O. "Effects of solvent and annealing on the improved performance of solar cells based on poly (3-hexylthiophene): Fullerene". Appl. Phys. Lett. 86 201120 (2005)

[16] Nalwa, H.S.; "Handbook of Organic Conductive Molecules and Polymers" Vol.3: "Conductive Polymers: Spectroscopy and Physical Properties" ISBN: 0-471-96595-2

[17] Tapany Udomphol, "Chapter 3- Elements of the theory of plasticity", Lecture 3, Suranaree University of Technology, (May-Aug 2007).

[18] Jordi Escarre, et al, "High Fidelity Transfer of Nanometric random textures by UV embossing for thin film solar cells applications", Solar Energy Materials and Solar Cells 95 pp: 881-886, (2011).

[19] Onobu Akogwu, David Kwabi, Swaminadham Midturi, Marcus Eleruja, Babaniyi Babatope, and W.O. Soboyejo, "Large strain deformation and cracking of nano-scale gold films on PDMS substrate ", Materials Science and Engineering B 170, pp: 32-40, (2010).

[20] Sokolnikoff, I. S., "Mathematical Theory of Elasticity", Second edition, McGraw-Hill Book Company, University of Califonia, Los Angeles, pp:100-101, (1956).

[21] Dieter, G.E., "Mechanical metallurgy", SI metric edition, McGraw-Hill, ISBN 0-07- 100406-8, pg: 69, (1988).

[22] http://pages.uoregon.edu/struct/courseware/461/461_lectures/461_l...

[23] Swaminadham Midturi, " STRESS-STRAIN BEHAVIOR OF NANO/MICRO THIN FILM MATERIALS", Donaghey College of Engineering and Infor-

mation Technology, University of Arkansas at Little Rock, Little Rock, USA, ARPN Journal of Engineering and Applied Sciences, VOL. 5, NO. 3, ISSN 1819-6608, ©2006-2010 Asian Research Publishing Network (ARPN), MARCH 2010, pg 72

[24] "ME 402 Experimental ME II – Three Point Bending Test", Yeditepe University Engineering Faculty, Mechanical Engineering Laboratory, pp 2-4

[25] http://en.wikipedia.org/w/index.php?title=Three_point_flexural_test&oldid=452418537

[26] http://www.sirim.my/plastics/flexuraltest.html

[27] http://www.mech.utah.edu/~rusmeeha/labNotes/composites.html

[28] Salters Horners, "Activity 20 - Bendy Wafer", Advanced Physics for Edexcel AS Physics. Essex, United Kingdom: Pearson Education. 2008.

[29] http://www.masonrysociety.org/Masonry%20Lab/Lab%203/Lab-3-four%20point.html

[30] Tom Markvart and Luis Castafier, Eds. "Solar Cells: Materials, Manufacture and Operation ", Copyright 2005, Elsevier Ltd., The Netherlands, pg: 32, (First edition 2005, Reprinted 2005, 2006).

[31] Paul A. Lane and Zakya H. Kafafi , "Solid-State Organic Photovoltaics: A Review of Molecular and Polymeric Devices ", Naval Research Laboratory, Washington, D.C., USA .

[32] Sam-Shajing Sun and Niyazi Serdar Sariciftci, "Organic Photovoltaics Mechanisms, Materials, and Devices", Copyright by Taylor & Francis Group, LLC, pp: 70- 76, (2005).

[33] Hiramoto, M.; Fujiwara, H., and Yokoyama, M. "p–i–n like behavior in three-layered organic solar cells having a co-deposited interlayer of pigments", J. Appl. Phys., 72(8), pp: 3781– 3787, (1992).

[34] Meier, H. "Organic Semiconductors", Verlag Chemie, Weinheim, pp: 372, 429, 459, (1974).

[35] Harima, Y.; Yamashita, K., and Suzuki, H. "Spectral sensitization in an organic p–n junction photovoltaic cell", Appl. Phys. Lett., 45(10), 1144–1145, (1984).

Chapter 3

[1] Onobu Akogwu, David Kwabi, Swaminadham Midturi, Marcus Eleruja, Babaniyi Babatope, and W.O. Soboyejo, "Large strain deformation and cracking of nano-scale gold films on PDMS substrate ", Materials Science and Engineering B 170, pp: 32-40, (2010).

Chapter 4

[1] Dieter, G. H., "Mechanical Metallurgy", SI metric edition, McGraw-Hill, ISBN 0-07- 1004006- 8, pg: 69, (1988).

[2] Odian, George, "Principles of Polymerization", 3rd ed., J. Wiley, New York, 1991.

[3] Jang, B. Z., "Advanced Polymer Composites: Principles and Applications", ASM International, Materials Park, OH, 1994.